Hydrogen storage mechanism and diffusion in metal–organic frameworks

Kenichi Koizumi, Katsuyuki Nobusada, Mauro Boero

Hydrogen storage mechanism and diffusion in metal–organic frameworks

Kenichi Koizumi,*,†,‡ Katsuyuki Nobusada,†,‡ and Mauro Boero¶

Department of Theoretical and Computational Molecular Science, Institute for Molecular Science, Myodaiji, Okazaki 444-8585, Japan, Elements Strategy Initiative for Catalysts and Batteries (ESICB), Kyoto University, Katsura, Kyoto 615-8520, Japan, and University of Strasbourg, CNRS, Institut de Physique et Chimie des Matériaux de Strasbourg UMR 7504, 23 rue du Loess, F-67034 Strasbourg, France

E-mail: koizumi@ims.ac.jp

Abstract

Diffusion and storage of hydrogen molecules in metal organic frameworks (MOF-5 and IRMOF-6) are crucial for the development of next-generation energy storage devices. By resorting to first principles modeling, we compute the diffusion coefficient of molecular hydrogen in these systems in a range of temperatures where MOF–based devices are expected to operate. The explicit inclusion of the electronic structure shows that diffusivities are one order of magnitude smaller than what reported by classical simulations, evidencing the insufficiency of the empirical force fields used so far. We show that hydrogen is mainly accumulated around the metal junction sites both in MOF-5 and IRMOF-6, and partly around the carbon atoms in

*To whom correspondence should be addressed

†Department of Theoretical and Computational Molecular Science, Institute for Molecular Science, Myodaiji, Okazaki 444-8585, Japan

‡Elements Strategy Initiative for Catalysts and Batteries (ESICB), Kyoto University, Katsura, Kyoto 615-8520, Japan

¶University of Strasbourg, CNRS, Institut de Physique et Chimie des Matériaux de Strasbourg UMR 7504, 23 rue du Loess, F-67034 Strasbourg, France

the case of IRMOF-6, where charged linkers are present. Metal ions embedded in the junction sites exert an electrostatic attraction toward hydrogen and the resulting distribution shows some ordering around these same sites at low temperature, whereas this tendency vanishes at room temperature. The induced polarization of hydrogen molecules generates an electrostatic interaction with charged atoms inside these nano-scaffolds and this is a key factor for the enhancement in hydrogen storage both in MOF-5 and IRMOF-6. The mechanism clarified hereby provides a novel understanding of metal organic frameworks and a guide to tune their efficiency for hydrogen storage. Moreover it paves the route to a computer-aided design of effective MOFs indicating that a fine control of the distribution of electrostatic charges inside the hydrogen hosting structure is crucial.

Introduction

Producing, handling and storing energy has become a priority in view of the increasing demand worldwide. Yet, this has to be sustainable and environmentally compatible. These fundamental issues must be accurately addressed for the realization of efficient and cost–competitive alternative power sources planned to be ready for the market by 2030.[1] In this context, hydrogen represents one of the most promising energy carrier and improvements in its storage are of primary importance.[2] One of the major difficulties is the fact that an H_2 gas easily diffuses and expands occupying a large volume. To overcome this problem, effective storage systems with good portability are necessary. Conventional storage methods require extremely high pressures which translates into heavy storage tanks for security issues and a relatively high energy consumption already at the stage of accumulation and production of a hydrogen reservoir. These two drawbacks are major stumbling blocks and call for the development of materials able to store large amounts of hydrogen at standard ambient conditions in a safe way.[3] A route pioneered in the last years is the storage inside solid materials sufficiently porous to allow H_2 to diffuse inside and able to exploit either physisorption or chemisorption mechanisms. To encourage developments in this direction, the U.S. Department of Energy (DOE) has set as a target the year 2020 for hydrogen storage for 5.5 wt% in gravimetric

capacity and 40 gL^{-1} of volumetric capacity at ambient temperatures and not extremely elevated pressure.[4] Metal-organic frameworks (MOFs) seem able to meet these requirements. In fact, they are sufficiently porus to accommodate appreciable amounts of H_2 molecules and rather versatile in realizing physisorption, as pioneered by Kondo[5] and Li.[6] In those exploratory works, microporous MOFs was synthesized and tested toward adsorption of different gases.[7] Since then, a variety of MOFs for hydrogen storages have been inspected.[8,9] Among all the available MOFs, MOF-5 is one of the best studied and more promising systems (Figure 1 a). This MOF consists of Zn_4O nodes with 1,4-benzodicarboxylic acid connecting the nodes[8] and has been shown to possess a storage ability for hydrogen of 7.1 wt% at 77 K.[10] Unfortunately, such a low temperature is a major drawback. Moreover, the storage capacity drops drastically to about 1.65 wt% at 298 K.[11] Indeed, this is the reason of the scarcity of experimental results for this class of systems in a temperature range closer to ambient conditions, conditions at which potential MOF–based devices are expected to operate. A second important system, IRMOF-6, is topologically similar to MOF-5, but includes a different organic linker, cyclobutylbenzene (Figure 1 b). Nonetheless, it has almost the same accessible volume of MOF-5[12] and can uptake an analogous amount of hydrogen at 77 K.[13,14] Yet, the behavior upon hydrogen storage at higher temperature is still a matter of debate.

To improve the hydrogen storage efficiency, avoiding the extreme cooling required, a detailed insight into the fate of H_2 molecules inside MOFs at room temperature is a mandatory first step. In this respect, molecular dynamics (MD) is a useful tool to investigate these processes at selected target temperatures. Yet, a reliable classical potential has to be selected and this is often not available for these complex systems. Classical MD simulations reported so far lack the inclusion of the electronic structure, which, instead, is a key ingredient to properly account for charge redistribution and dynamical change of relevant chemical bonds inside the network. To cope with this intrinsic difficulty, we resort to first-principles molecular dynamics (FPMD) to describe the various diffusion processes of hydrogen molecules inside MOF structures. FPMD has been assessed and benchmarked on a wide variety of systems where diffusion processes are essential, from solids,[15–18] to surfaces,[19–21] as well as liquids[22–27] and gases.[28,29] Recent advances in high

performance computers (HPCs) for massively parallel calculations and softwares developments are already mature to allow simulations of dynamical process for systems composed by more than 500 atoms. On these grounds, we report a detailed investigation of diffusion processes of H_2 inside both MOF-5 and IRMOF-6 at a full FPMD level which is still lacking and has so far never been afforded at a FPMD level. Diffusion coefficients are computed at various temperatures upon statistically significant simulation times. The temperature dependence in the distribution of H_2 molecules inside the MOF-5 is clarified, allowing for a rationalization of the degradation in hydrogen storage performances of this system. We also show that the dynamical behavior hydrogen molecules in MOF-5 and IRMOF-6 is quite different at room temperature. Diffusion coefficients in IRMOF-6 turn out to be significantly smaller than in MOF-5. Neutron diffraction experiments[30] allowed to speculate that ionic metal junction sites should be the preferred H_2 uptaking site at least at extremely low temperature (3.5 K). Those exploratory works reported a cage like ordering in the distribution of H_2 molecules in proximity of metal junction sites. Classical MD simulations[31] confirmed the pivotal role of these same sites as H_2 captors at 77K in MOF-5. However, because of the limitations of classical MD mentioned above, a clear insights into the diffusion process, the subtle electronic structure modifications and the effects of higher temperature up to ambient conditions have never been elucidated. Here, we fill this gap by showing, via FPMD, the effect of temperature in the molecular hydrogen distribution inside the frameworks and the persistence of the attractive character of metal junction sites even at room temperature. Some ordering in the distribution of molecular hydrogen still exists at 200K, whereas this tendency vanishes at 300K. Moreover, we show that electrostatic interaction between H_2 molecules and the exposed surface inside MOFs is crucial for hydrogen storage. In fact, the local electrostatic potential is affected by the redistribution of the charge density within the framework, an effect completely neglected in classical MD approaches. The charges of the residues introduced in the organic linkers of MOFs also affect strongly the hydrogen diffusion processes. These insights provide precious guidelines for the design of effective MOFs system via the control of the electrostatic charges present not only on the metal junction sites, only focus of all previous works, but also in the organic linkers

introduced in the frameworks.

Computational Methods

The simulated structures of MOF-5 and IRMOF-6 are shown in the two upper panels of Figure 1, along with their respective linkers in the insets. Specifically, the first one has a 1,4-benzenedicarboxylate (BDC) linker, whereas the second one an R_6-BDC and both ensure the connection to the Zn ions. These sites are the one refereed to as "metal junction sites" hereafter. At this specific locations, evidenced by a white circle in the upper panels of Figure 1, O atoms of carboxy groups belonging to the organic linkers are bound to Zn.

In both MOFs, Zn ions of the metal junction sites are deeply embedded inside the framework and as such barely exposed to potentially adsorbed molecules. The formulas for the simulation cells used in our calculations are $C_{192}H_{96}O_{104}Zn_{32}$ for MOF-5 and $C_{240}H_{144}O_{104}Zn_{32}$ for IRMOF-6. Periodic boundary conditions are adopted for all simulated systems. Since the reported amount of the hydrogen storage in MOF-5 is 1.65wt% at 298K,[11] we adjusted consistently the amount of H_2 molecules added inside our system. This translates into 52 H_2 molecules inside the simulation cell of MOF-5 and 51 for the IRMOF-6 system, both being cubic supercells of lateral size equal to 25.8 Å. The total number of atoms for the two cases becomes then 528 for MOF-5 and 622 for IRMOF-6. and Figure 1 illustrates in panels a and b our two simulates systems.

Our FPMD simulation scheme is based on the unified approach of density-functional theory (DFT)[32,33] and MD originally presented by Car and Parrinello.[34] Valence electrons wavefunctions are represented on a plane-wave basis set with an energy cut-off of 80 Ry and the Brillouin zone sampling is limited to the Γ point. The Perdew-Burke-Ernserhof (PBE)[35] generalized gradient approximation (GGA) is adopted for the exchange-correlation interaction.[35] To account for long range van der Waals interactions, not included in any GGA, we use the Grimme's empirical correction D2.[36] The core-valence interactions are described by Troullier-Martins norm-conserving pseudopotentials.[37] The integration time step was 0.096 fs (4.0 atomic unit), and the fictitious

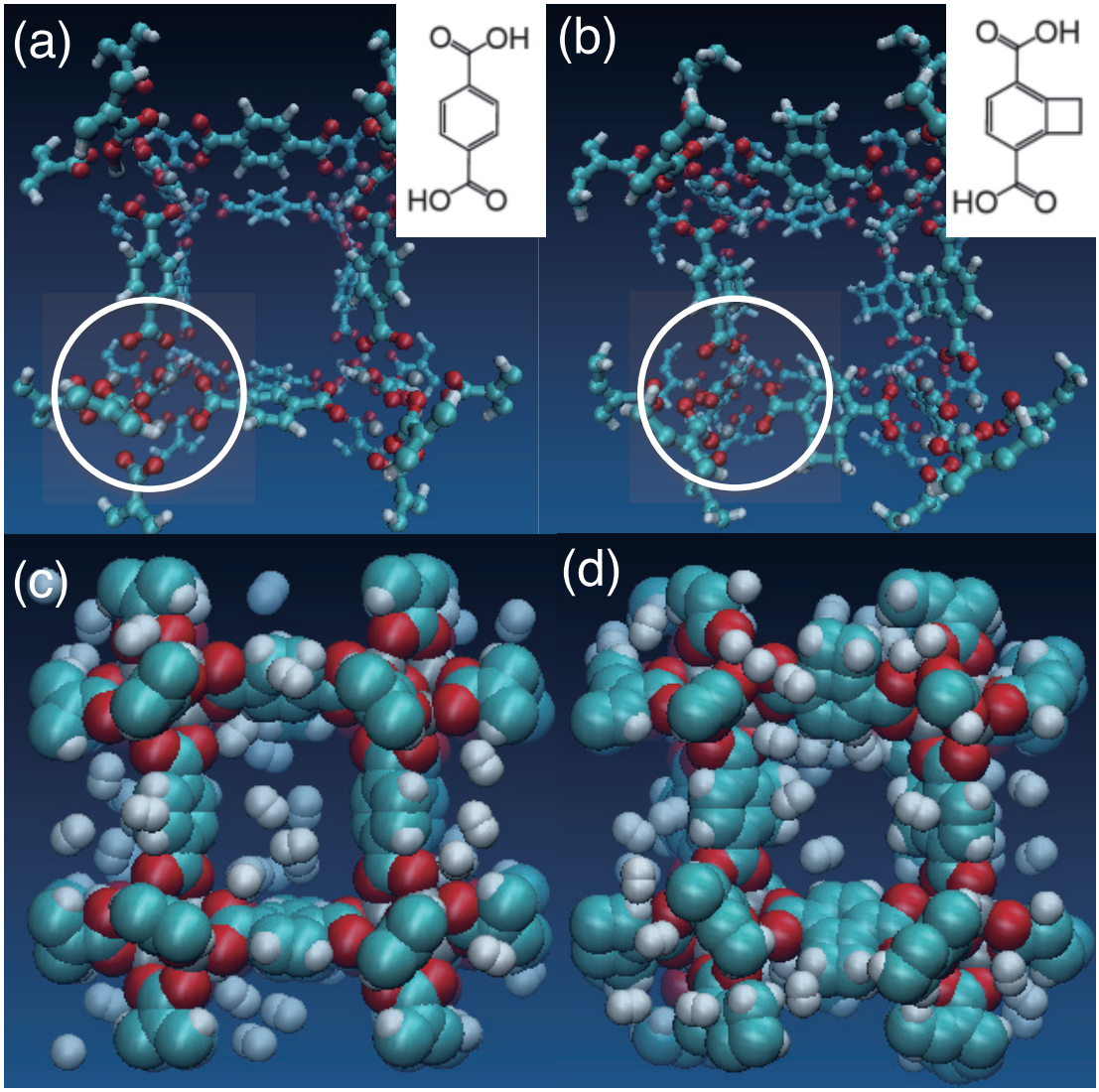

Figure 1: Structural models of MOF-5 (a) and IRMOF-6 (b) used in our simulations. The insets show the organic linkers of MOF-5 and IRMOF-6, namely BDC and R_6-BDC. The white circle indicate one of metal junction site where the carboxyl groups of the linkers BDC or R_6-BDC are connected to Zn. Panels (c) and (d) show two snapshots taken during the MD simulations of MOF-5 and IRMOF-6 (d), respectively and the size of the spheres reflects the van der Waals radius of each atomic species. The color code is cyan for C, red for O, gray for Zn, and white for H. 52 and 51 H_2 molecules are included in the MOF-5 and IRMOF-6 simulation cells.

electronic mass was set to μ=400.0 atomic units, which ensures a good control of the conserved quantities.[38] The ionic temperature is controlled by a Nosé-Hoover chain thermostat and dynamical simulations are performed in the canonical NVT ensemble.[39–42] Different temperatures corresponding to 200, 300, 400, and 500 K are considered in the case of MOF-5 and 200 K is the target temperature used for the case of IRMOF-6. About 10 ps MD was necessary to fully equilibrate the systems, then statics were collected in the following 19.2 ps (about 200000 MD steps). We used the CPMD package for all simulations.[43]

Results and Discussions

Hydrogen Diffusion inside MOFs

A rather long–lasting FPMD simulation was performed within the approach specified above. During a simulation time of 19.2 ps, after the full equilibration of the system, we accumulated statistics and computed the mean square displacement (MSD) $\Delta R^2(t)$ according to the standard formula

$$\Delta R^2(t) = \frac{1}{N}\sum_{i=1}^{N} |\boldsymbol{R}_i(t) - \boldsymbol{R}_i(0)|^2 \tag{1}$$

where N is the number of hydrogen molecules in the system and $\boldsymbol{R}_i(t)$ the position of the center of mass of the i^{th} H_2 molecule at time t. The result of this analysis is summarized in Figure 2, showing the MSDs of MOF-5 at the various temperatures considered, along with the MSD at 200 K in the case of IRMOF-6.

Since our simulations started from a well equilibrated conditon and the statistics was collected for a relatively long time, all MSDs display a linear trend suitable to estimate the diffusivities. Indeed, as shown in Figure 2, a linear fitting of the crude $\Delta R^2(t)$ as a function of the time gives straight lines nearly indistinguishable from the computed data. By using the Einstein relation,

$$\Delta R^2(t) = 6D \cdot t + \Delta R^2(0). \tag{2}$$

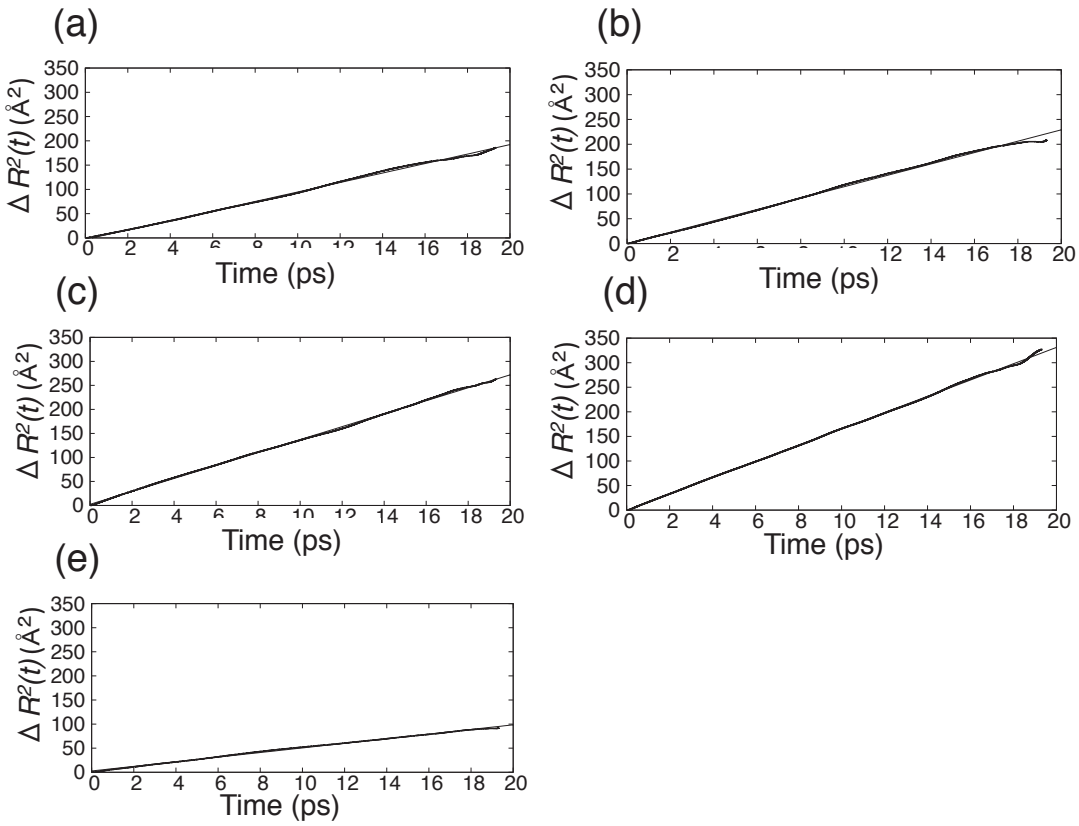

Figure 2: Mean squared displacements for the diffusions of H_2 molecules inside the MOF-5 system at 200 (a), 300 (b), 400 (c) and 500 K (d), respectively. Panel (e) show the analogous mean squared displacement for IRMOF-6 at 200 K. The straight thin lines show the linear least square fitting and the thicker black lines the actual values computed from the displacement of the centers of mass of each hydrogen molecule.

we computed the diffusion coefficient D, for which all values are summarized in Table.1 and the trend as a function of the temperature is reported in Figure 3. For the sake of completeness, we have added to the plot also the classical MD result of Skoulidas and Sholl.[44]

Table 1: Diffusion coefficients (cm^2/s) of the hydrogen molecules inside MOF-5 (a) and IRMOF-6 (b), respectively.

(a)	
T (K)	Diffusion coefficient (cm^2/s)
200	1.63×10^{-4}
300	1.91×10^{-4}
400	2.25×10^{-4}
500	2.76×10^{-4}
(b)	
T (K)	Diffusion coefficient (cm^2/s)
200	7.98×10^{-5}

As Figure 3 shows, the diffusion coefficient of MOF-5 follows a nearly perfect Arrhenius behavior at least for the range of temperatures investigated. Yet, the values computed appear to be quite large in comparison with available experimental data on hydrogen diffusion in zeolites ($\sim 1.0 \times 10^{-8}$ cm^2/s),[45] but, at the same time, about two order of magnitude smaller than diffusion coefficients in single-wall carbon nanotubes, at least according to classical MD simulations ($\sim 1.0 \times 10^{-2}$ cm^2/s).[46] This is not so surprising in view of the overestimation affecting typical classical MD simulations, as shown in Figure 3. Indeed, since classical simulations do not account for the electronic degrees of freedom and charge density redistribution processes, such as the polarization acquired by H_2 molecules upon adsorption, it seems that a crucial part of the electrostatic interaction is missing in standard force fields. This is likely to be the source of the overestimation mentioned above. On the contrary, by accounting explicitly for the electronic structure, as done in this work, diffusivities result to be ten times smaller than what has been proposed.[44] This shows the importance of an accurate inclusion of the electronic degrees of freedom in the description of the diffusion processes. From our Arrhenius plot, we can also extract the migration energy for H_2

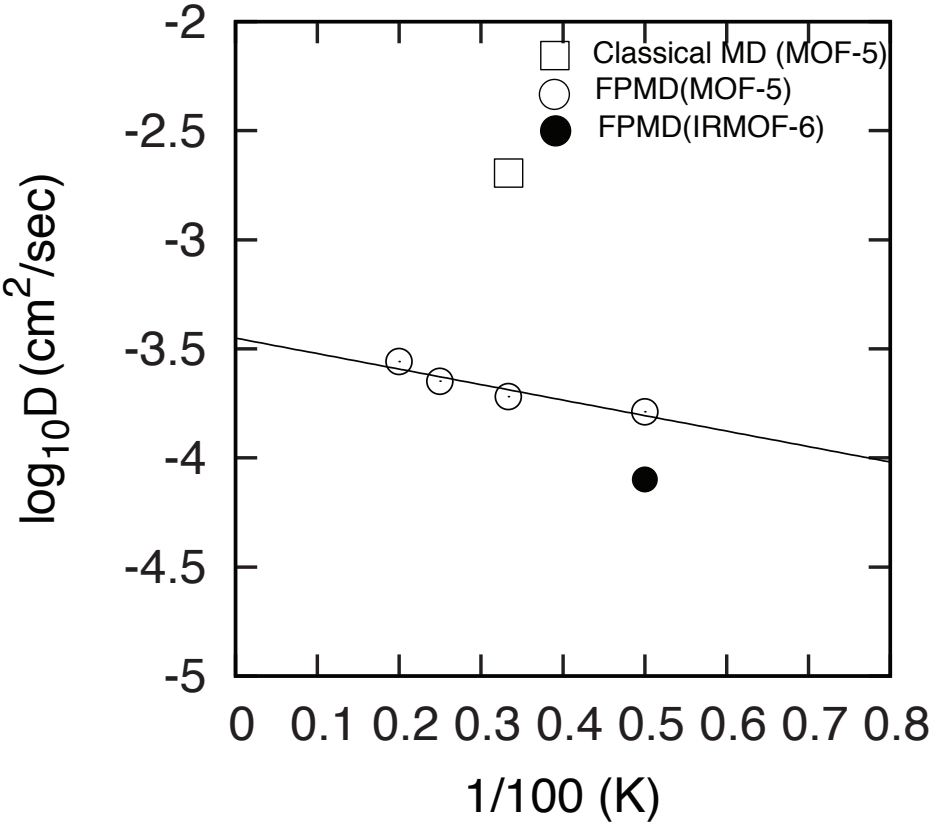

Figure 3: Diffusion coefficient of hydrogen molecules inside MOF-5 and IRMOF-6. The classical molecular dynamics result reported is taken from Ref.[44]

molecules, which turns out to be 0.014 eV for MOF-5.

Spatial distribution of molecular hydrogen

The dynamical evolution of H_2 molecules during the FPMD simulation provides also a sufficiently long exploration of the regions accessible to molecular hydrogen inside the framework. On these grounds, we mapped the spatial distribution of H_2 molecules in MOF-5 at the various temperatures at which NVT simulations have been conducted. To rationalize such a mapping, simulation supercells have been partitioned into a mesh of $30\times30\times30$ small cubic boxes, each one having a lateral size of about 0.86 Å. Such a fine subdivision ensures that each small box contains just one H_2 molecule. On the basis of this space subdivision, we counted the number of times a hydrogen molecule visits each small cube along the FPMD trajectories. The resulting spatial distribution maps are shown in Figure 4. This statistics has been constructed on the basis of upper bound values. Specifically, if a molecule visits 200 times a given small cubic box distributions of panels a, c and e in that figure are the resulting statistics, whereas panels b, d and f are the distribution in the case of 300 times visits. These values are not randomly chosen. On the contrary, they give an estimate of the resident time of molecular hydrogen. In fact, along our FPMD simulations, trajectories were stored each ten steps and, with our choice of time step (0.096 fs), these integer numbers translate into 2 and 3 ps, namely 1% and 1.5% of total simulation time, respectively.

A first message that panel a of Figure 4 conveys is that H_2 molecules distribute mainly around the metal junction sites, at the corners of the MOF-5 structure at 200 K. This is consistent with the results reported for extremely low temperatures (3.5 K) by neutron diffraction experiments[30] and shows that this trend still holds also at higher values approaching room temperature. Upon increasing the temperature, as shown in panels c and d, H_2 molecules show a tendency to move toward the pore of the framework. Simultaneously, (see panel c) a decrease in the distributions around the metal junction sites occurs, as a consequence of the fact that molecular hydrogen starts populating the pores at 300 K. In the same figure, a comparison of panels a and b shows, in the latter case, that H_2 molecules tend to accumulate around the metal junction sites on longer observation

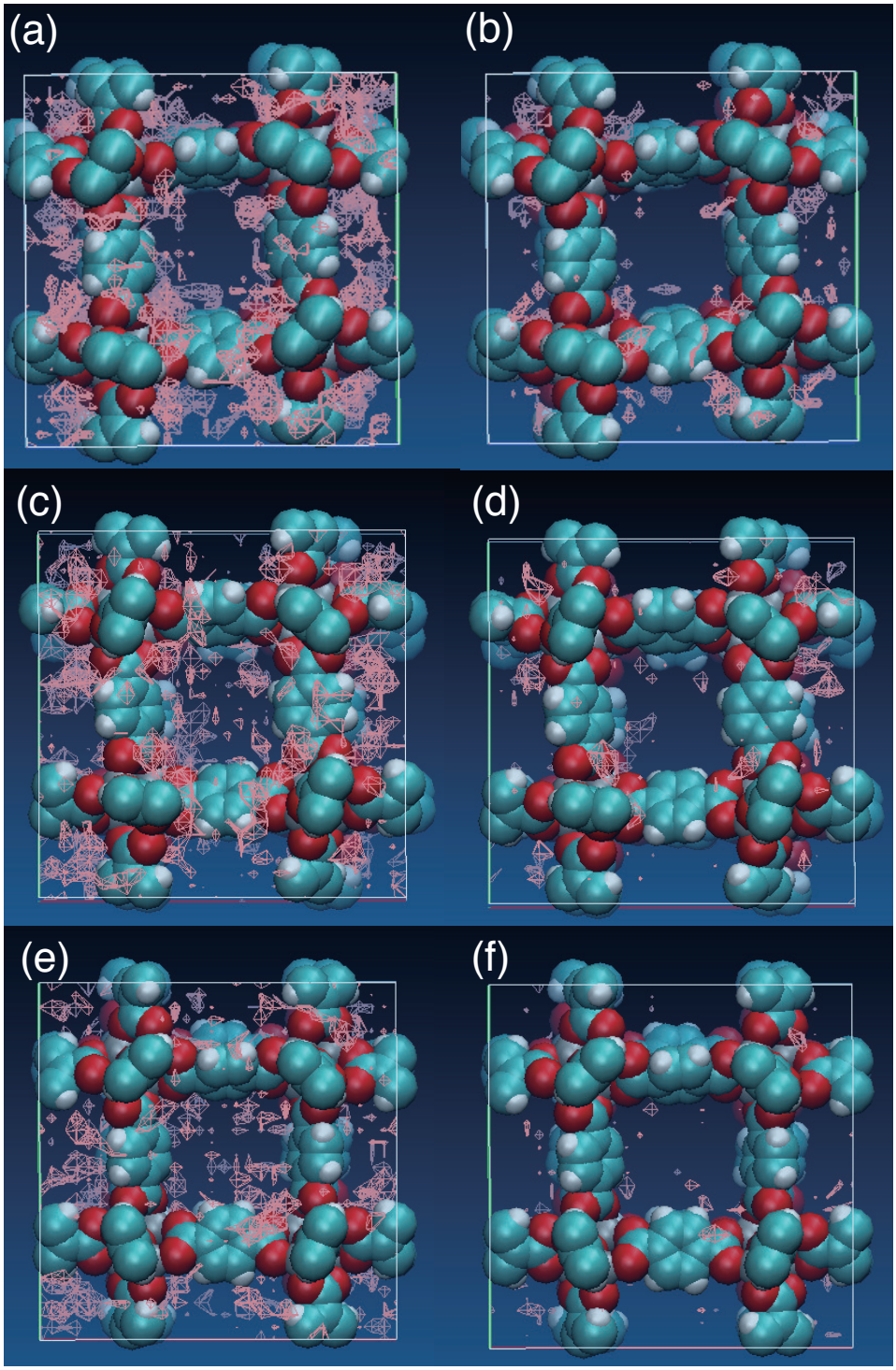

Figure 4: Spatial distribution of hydrogen molecules inside MOF-5. Panels (a) and (b) refer to 200 K and residence times of 2 and 3, panels (c) and (d) refer to 300 K and residence times of 2 and 3 ps, panels (e) and (f) are the distributions at 500 K for residence times of 2 and 3 ps, respectively. Details are given in the text. The color code for atoms is identical to the one used in Figure 1.

times. This feature is a clear indication that molecular hydrogen localizes most of the time around these specific sites, which become the preferred accumulation points inside the framework. This feature changes remarkably at higher temperature, as evidenced, in descending order in Figure 4, by panels d and f if we consider longer residence times. In particular, at high temperatures (panel f) the barrier for H_2 physisorption is easily overcome by the thermal kinetic energy at 500 K. A key point that we learn from these results is that having metal junction sites with strong affinity to hydrogen is a fundamental requirement in the design of MOF–based devices able to operate at ambient temperature and above, especially in view of the heat developed by the processes of accumulating and delivering hydrogen and, consequently, energy.

In the case of IRMOF-6 at 200 K, by adopting the 2 ps upper bound as a residence time, the distribution around the R_6-BDC moieties becomes rather evident, as seen in Figure 5 a. By assuming as the time upper limit the 3 ps threshold, H_2 molecules appear to accumulate both around the metal junction sites and the R_6-BDC moieties. This is another important indication in the design of MOF systems, namely the introduction of charged residues in organic linkers become a new attractive site for molecular hydrogen, thus enhancing the storage ability of the framework.

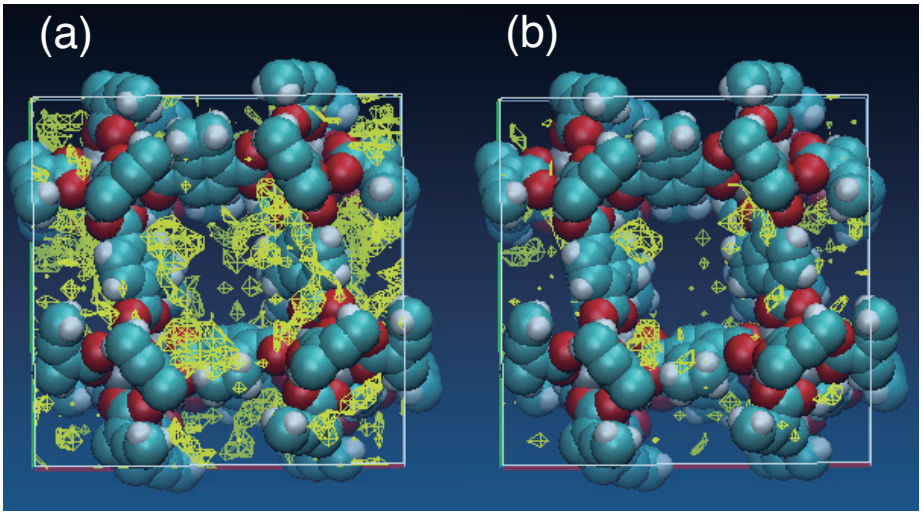

Figure 5: Spatial distribution of hydrogen molecules inside IRMOF-6 at 200 K. The counting thresholds for (a) and (b) are 200 (1% of the total time) and 300 times (1.5% of the total time) in each small cubic box in which the system has been partitioned, as explained in the text. The color code for atoms is identical to the one used in Figure 1.

To get a better insight into the displacement of molecular hydrogen inside the MOF-5 system, we monitored the distance of H_2 molecules from the Zn and O atoms at a metal junction site along the dynamical trajectory. Ten of these distances are shown in Figure 6 as a function of the simulation time. In this figure, panel a shows the evolution of the distances between these H_2 molecules and the O site in the metal junction, whereas panel b shows the evolution of the distances between these same H_2 molecules and the Zn atom. In both cases, hydrogen molecules seem unable to approach either O or Zn to a distance shorter then 3.0 Å. On the contrary, H_2 molecules spend most of the time away from these specific sites and when they approach, they leave rather quickly. This analysis of the instantaneous H_2 positions is corroborated by the distributions discussed above and underscore the fact that Zn and O sites are not prone to uptake molecular hydrogen.

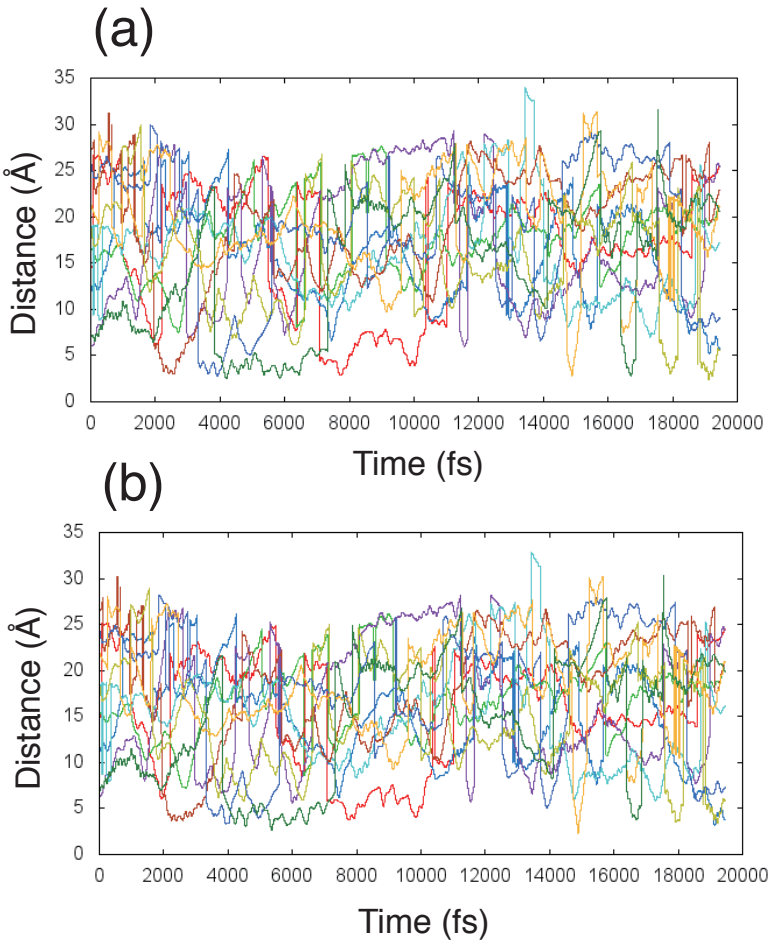

Figure 6: Distances of ten representative H_2 molecules from the Zn (a) and O (b) atoms belonging to a metal junction site. The Zn and O atoms are located in neighboring positions.

To quantify these features, we computed the radial distribution function (RDF) of the H_2 molecules from the Zn, O and H atoms located in the metal junction sites of the MOF-5 system at 200 and 300 K. The result obtained is shown in Figure 7 and we remark that all the H atoms considered in this case belong to benzene moieties

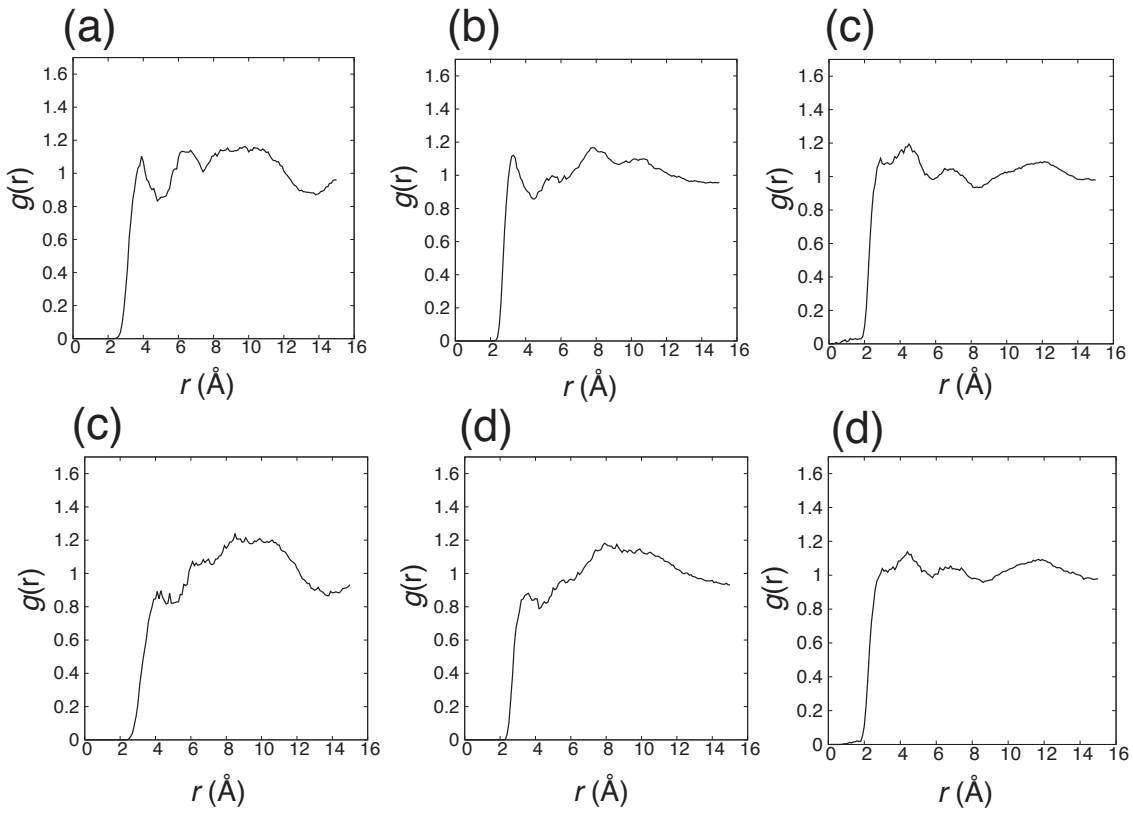

Figure 7: Radial distribution functions of hydrogen molecules from the Zn (a), O (b) and H (c) atoms in MOF-5 at 200 K. Analogous distributions at 300 K are the ones in panels (c), (d), and (e), respectively.

By looking at panels a and b, a first feature that can be remarked is a sharp peak at 3.0 Å in the case of Zn and O. This indicates that at 200 K an accumulation of molecular hydrogen occurs around these sites. This is in fair agreement with the results reported by Yildirim and Hartman at extremely low temperature (3.5 K).[30] So the hydrogen uptaking trend in the vicinity of the metal junction site is preserved at 200 K. On the other hand, the RDF of the benzene-like H atoms in panel c does not show any appreciable feature at short distance but an unclear shoulder. So, these H atoms cannot be regarded as potential accumulation sites. Conversely, at room temperature (300

K), the sharp peaks around 3.0 Å from the origines disappear (panels c and d) and both Zn and O sites are then no longer H_2 accumulation sites. The number of hydrogen molecules distributed around the Zn and O atoms at increasing distances r can be computed by integrating the RDFs $g(r)$, namely

$$N(r) = 4\pi \int_0^r r'^2 \rho g(r') dr'. \quad (3)$$

Where ρ indicates the average density of the H_2 molecules in the simulation cell. The result of this integration is summarized in Table 2.

Table 2: Number of hydrogen molecules around O (a) and Zn (b) atoms at increasing distances obtained upon integration of the corresponding radial disitribution functions.

(a)		
Distance (Å)	Number of molecules (200 K)	Number of molecules (300 K)
4.0	0.59	0.49
5.0	1.28	1.14
6.0	2.42	2.24
(b)		
Distance (Å)	Number of molecules (200 K)	Number of molecules (300 K)
4.0	0.45	0.33
5.0	1.16	0.99
6.0	2.27	2.06

We found that, on average, at least one or two H_2 molecules are distributed around the Zn and O atoms at 200 K, the temperature at which these sites still act as attractors to molecular hydrogen. However, this number rapidly decreases by increasing the temperature to 300 K and by integrating the RDFs up to identical radial distances (5 Å), which, we remind, do no longer correspond to a clear RDF minimum. It seems that at 300 K the thermal motion of Zn and its surrounding atoms makes the metal more embedded and shielded so that it becomes unable to uptake H_2 molecules. Moreover, even at low temperature, the distances at which H_2 molecules seem to be accumulated (3-4 Å) is slightly larger than what reported using static calculations on model complexes constructed ad hoc to simulate these metal junction sites,[47,48] a fact that seem

to underscore the insufficiency of static approaches and smaller models not accounting for the complexity of the MOF structure as a whole.

Charge density redistribution and hydrogen displacement

To get a deeper insight into the role of the electronic charge and its redistribution in the process of diffusion and accumulation of molecular hydrogen inside a MOF system, we extracted uncorrelated configurations from the trajectories of MOF-5 and IRMOF-6 and computed the charge density differences according to the expression

$$\Delta\rho = \rho(\mathrm{H_2\ molecules + MOF}) - (\rho(\mathrm{H_2\ molecules}) + \rho(\mathrm{MOF})) \tag{4}$$

and the result is reported graphically in Figure 8.

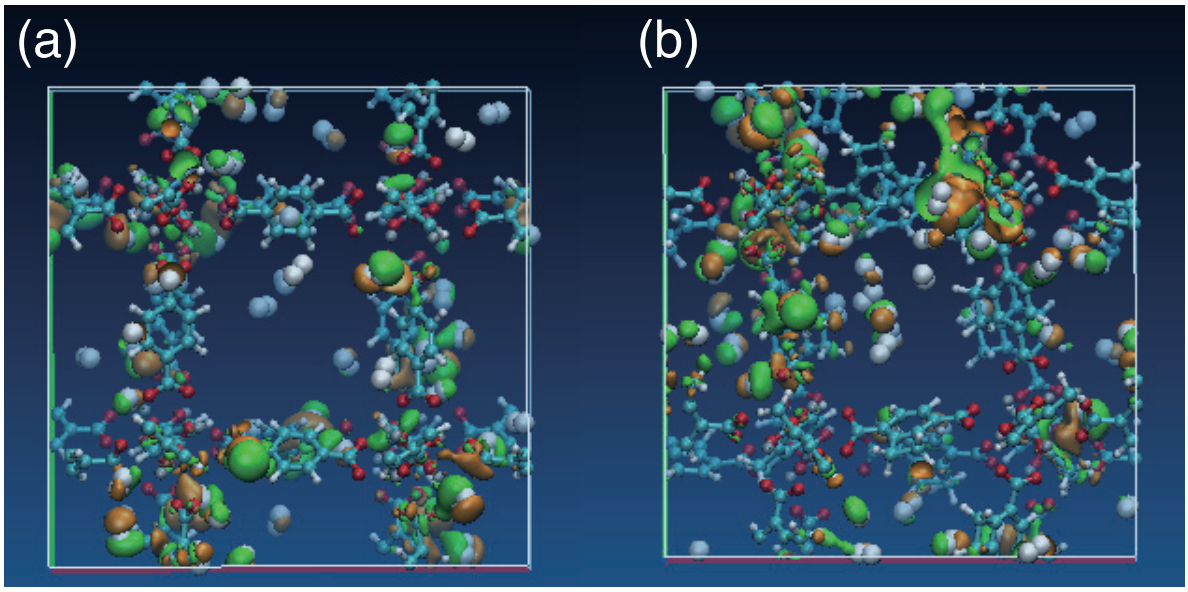

Figure 8: Charge density differences for MOF-5 (a) and IRMOF-6 (b). Green and orange colors indicate an increase and a decrease of charge density, respectively. Isosurfaces are shown at a value of $\pm 1.0 \times 10^{-4}$ e/Å^3. The color code for atoms is identical to the one used in Figure 1.

In the case of MOF-5, the values of $\Delta\rho$ around H_2 molecules located in the vicinity of the metal junction sites shows two lobes of different colors, hence an increase and a decrease of electronic charge on the two opposite sides of the hydrogen molecule. This is a clear signature of a

polarization effect that H_2 molecules experience upon approaching the metal junction sites. For comparison, all other H_2 molecules inside the pore and far from the junction sites are not polarized as the absence of any $\Delta\rho$ confirms. Another noticeable feature is the increase of charge density around O atoms belonging to the carboxy groups and in the vicinity of the Zn ions. All these charge redistribution features concur in completing the picture and show that the strong polarization of molecular hydrogen is a key factor in the process of hydrogen uptake. Indeed, an analysis of the displacement of the H_2 molecules inside MOF-5 during the dynamics provides a further confirmation of this conclusion. By looking at the trajectory of a representative H_2 molecule in panel a of Figure 9, it is evident that although nothing prevents the molecule to migrate inside the pore and center of MOF-5, the molecular hydrogen prefers to migrate along the framework and spends most of its time around the metal junction sites. In view of the charge polarization effects discussed above, we can infer that local electrostatic effects due to the charge redistribution play a major role in driving and, to a certain extent, constraining the hydrogen migrations inside the system.

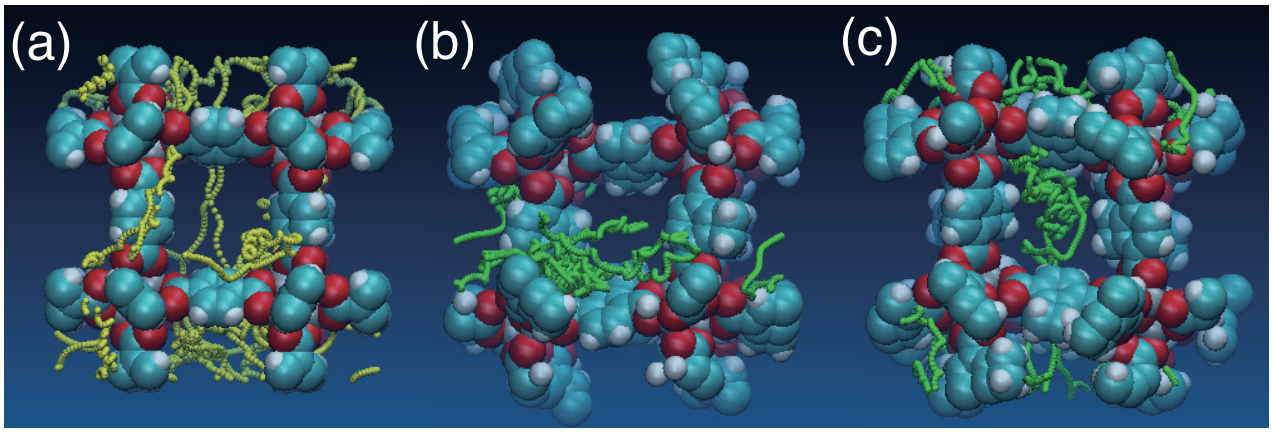

Figure 9: Trajectory of hydrogen molecules inside MOF-5 represented as a sequence of small yellow spheres (a) and inside IRMOF-6 in panels (b) and (c), each one referring to a different H_2 molecule and represented as a sequence of small green spheres. The trajectories of the molecules are in each case subject to periodic boundary conditions and have not to be interpreted as broken on the cell borders. The color code for atoms is identical to what has been used in Figure 1.

Analogously, also in IRMOF-6 polarized H_2 molecules appear around the R_6-BDC moieties (Figure 8 b). A sign that the local electrostatics is deeply affected by the interaction between

molecular hydrogen and the framework. On the contrary, H_2 molecules far from both the R_6-BDC moieties and the metal junction sites do not show any polarization. However, an analysis of the diffusion of hydrogen molecules inside the system (Figure 9 b, c) reveals that H_2 molecules can move also inside the pore, whereas parts of them still prefers to stay bound to the R_6-BDC moieties. This is not totally unexpected on the basis of the RDFs. To get a better insight into the local electrostatic modifications, we computed the Mulliken charges of the C atoms belonging to the cyclobutane rings in the R_6-BDC moieties. The values of these charges on the two C atoms exposed to the approaching hydrogen molecules have values of 0.26–0.35, remarkably different from the remaining C atoms and C sites of the benzene rings, which display negligible values ranging between 0.01 and 0.02. For comparison, also in the case of benzene moieties in MOF-5 the Mulliken charges of the carbon sites are in the same range (0.01–0.02), indicating a negligible polarization. We can then infer that the rather large charges of the exposed C atoms induce a polarization of the approaching H_2 molecules, thus making the R_6-BDC groups of IRMOF-6 attractor sites for the molecular hydrogen. The polarization of H_2 molecules, in turn, affects substantially the diffusion inside the frameworks of both MOF-5 and IRMOF-6. All these subtle aspects escape classical MD simulations and all of them can be rationalized only in terms of local electronic structure modifications, thus calling for FPMD approaches. Furthermore, these FPMD simulations show rather clearly that the charged residues present in the linkers influence drastically the diffusion processes of molecular hydrogen inside the systems, thus providing a fundamental understanding in the mechanism regulating the storage and release.

Conclusions

Our FPMD simulations offer a clear picture of the diffusion mechanism of hydrogen molecules in MOF-5 and IRMOF-6 at temperatures higher than what is generally reported. This is crucial in view of the use at ambient temperature of potential devices based on these materials. At variance with former simulations neglecting the electronic structure and its modifications, we show

that diffusion coefficients are at least one order of magnitutde smaller than what has been so far believed on the basis of classical MD simulations. Since classical force fields are unable to accurately describe local electrostatic modifications and polarizations evolving in time, diffusivities estimated within these approaches turn out to be a rough overestimation. An analysis of the probability of the spatial distributions of H_2 molecules inside the frameworks shows that metal junction sites in MOF-5 act as attractor centers for molecular hydrogen up to room temperature (300 K). Conversely, at higher temperature (500 K), these sites are no longer good H_2 attractors and this can compromise devices based on MOF-5, since high temperatures are likely to be reached upon heating resulting from the energy storage and delivery processes. On the other hand, the same analysis shows that the charged R_6-BDC moieties of IRMOF-6 exert additional attraction toward H_2 molecules, making this material more promising. An clear indication that can be extracted is the fact that charged residues included in the organic linker act as additional attractors for H_2 and influence their diffusion. Analyses of the charge density modifications show that hydrogen molecules in proximity of charged sites become polarized and this influences the diffusion and migration of H_2 molecules, which tend to localize around these sites. The radial distribution functions display some ordering in the spatial distribution of molecular hydrogen around O and Zn atoms in the metal junction sites, at least for temperatures lower than 300 K. The information provided by this analysis is that despite the fact that Zn atoms are rather embedded inside the junction, they are still able to attract H_2 molecule. This feature, however is lost at 300 K.

On the basis of our study, we propose that a key factor for improving hydrogen storage in MOF systems is a careful addition of charged groups in the structure, which are able to stimulate the polarization of H_2 molecules and thus their uptaking. The charged residues are at least as crucial as the metal ions. Hence, a careful design of the metal organic frameworks and a tuning of the distribution of the electrostatic charges within the structure can pave the route to the realization of efficient next-generation energy storages and delivery MOF–based devices.

References

(1) Full documentation at
https://ec.europa.eu/energy/en/topics/energy-strategy-and-energy-union/2030-energy-strategy
and
http://www.climateactionprogramme.org/news/japan_on_track_to_reach_35_renewables
_by_2030

(2) Coontz, R.; Hanson, B. Not So Simple. *Science* **2004**, *305*, 957

(3) Zuttel, A. Materials for Hydrogen Storage. *Materials Today* **2003**, *6*, 24-33

(4) Eds. Tayde, R. J.; Gandhi, V. *Photocatalytic Nanomaterials for Environmental Applications* Materials Research Forum LLC, **2018**

(5) Kondo, M.; Yoshitomi, T.; Seki, K.; Matsuzaka, H.; Kitagwa, S. Three-Dimensional Framework with Channeling Cavities for Small Molecules: $\{[M2(4, 4'\text{-bpy})_3(NO_3)_4]xH2O\}_n$ (M = Co, Ni, Zn). *Angew. Chem. Int. Ed.* **1997**, *36*, 1725-1727

(6) Li, H.; Eddaoudi, M.;Groy, T. L.;Yagi, O. M. Establishing Microporosity in Open Metal–Organic Frameworks: Gas Sorption Isotherms for Zn(BDC) (BDC = 1,4-Benzenedicarboxylate) *J. Am. Chem. Soc.* **1998**, *120*, 8571-8572

(7) Li, H.; Eddaoudi, M.;O'Keeffe, M.;Yaghi,O. M. Design and Synthesis of an Exceptionally Stable and Highly Porous Metal-Organic Framework. *Nature* **1999**, *402*, 276-279

(8) Rosi, N. L.; Eckert, J.; Eddaoudi, M.; Vodak, D. T.; Kim, J.; O'Keeffe, M.; Yaghi, O. M. Hydrogen Storage in Microporous Metal-Organic Frameworks. *Science* **2003**, *300*, 1127-1129

(9) Murray, L.; Dinca, M.; Long, J. R. Hydrogen Storage in Metal–Organic Frameworks. *Chem. Soc. Rev.* **2009**, *38*, 1294-1314

(10) Kaye, S. S.; Dailly, A.; Yaghi, O. M.; Long, J. R. Impact of Preparation and Handling on the Hydrogen Storage Properties of Zn_4O(1,4-benzenedicarboxylate)$_3$ (MOF-5) *J. Am. Chem. Soc.* **2007**, *129*, 14176-14177

(11) Pan, L.; Sander, M. B.; Huang, X.; Li, J.; Smith, M.; Bittner, E.; Bockrath, B.; Johnson, J. K. Microporous Metal Organic Materials: Promising Candidates as Sorbents for Hydrogen Storage. *J. Am. Chem. Soc.* **2004**, *126*, 1308-1309

(12) Eddaoudi, M.; Kim, J.; Rosi, N.; Vodak, D.; Wachter, J.; O'Keeffe, M.; Yaghi, O. M. Systematic Design of Pore Size and Functionality in Isoreticular MOFs and Their Application in Methane Storage. *Science* **2002**, **295**, 469-472

(13) Wong-Foy, A. G.; Matzger, A. J.; Yaghi, O. M. Exceptional H_2 Saturation Uptake in Microporous Metal–Organic Frameworks. *J. Am. Chem. Soc.* **2006**, *128*, 3494-3495

(14) Rowsell, J. L. C.; Yaghi O. M. Effects of Functionalization, Catenation, and Variation of the Metal Oxide and Organic Linking Units on the Low-Pressure Hydrogen Adsorption Properties of Metal–Organic Frameworks. *J. Am. Chem. Soc.* **2006**, *128*, 1304-1315

(15) Koizumi, K.; Boero, M.; Shigeta, Y.; Oshiyama, A. Self-Diffusion in Crystalline Silicon: A Car-Parrinello Molecular Dynamics Study. *Phys. Rev. B* **2011**, *84*, 205203

(16) Tuckerman, M. E.; Klein, M. L. *Ab Initio* Molecular Dynamics Study of Solid Nitromethane. *Chem. Phys. Lett.* **1998**, *283*, 147-151

(17) Sullivan, D. M.; Bagchi, K.; Tuckerman, M. E. *Ab Initio* Molecular Dynamics Study of Crystalline Nitric Acid Trihydrate. *J. Phys. Chem. A* **1999**, *103*, 8678-8683

(18) Boero, M.; Oshiyama, A.; Silvestrelli, P. L.; Murakami, K. Free energy molecular dynamics simulations of pulsed-laser-irradiated SiO_2: Si–Si bond formation in a matrix of SiO_2. *Appl. Phys. Lett.* **2005**, *86*, 201910

(19) Koizumi, K.; Boero, M.; Shigeta, Y.; Oshiyama, A. Microscopic Mechanisms of Initial Oxidation of Si(100): Reaction Pathways and Free-Energy Barriers. *Phys. Rev. B* **2012**, *85*, 205314

(20) Koizumi, K.;Boero, M.;Shigeta, Y.; Oshiyama, A. Atom-Scale Reaction Pathways and Free-Energy Landscapes in Oxygen Plasma Etching of Graphene. *J. Phys. Chem. Lett.* **2013**, *4*, 1592–1596

(21) Koizumi, K.; Nobusada, K.; Boero, M. An Atomic-Level Insight into the Basic Mechanism Responsible for the Enhancement of the Catalytic Oxidation of Carbon Monoxide on a Cu/CeO_2 Surface. *Phys. Chem. Chem. Phys.* **2017**, *19*, 3498–3505

(22) Boero, M.; Ikeshoji, T.; Terakura, K. Density and Temperature Dependence of Proton Diffusion in Water: A First-Principles Molecular Dynamics Study. *ChemPhysChem* **2005**, *6*, 1775-1779

(23) Laasonen, K.; Sprik, M.; Parrinello, M.; Car, R. "*Ab Initio*" Liquid Water. *J. Chem. Phys.* **1993**, *99*, 9080-9089

(24) VandeVondele, J.; Mohamed, F.; Krack, M.; Hutter, J.; Sprik, M.; Parrinello, M. The Influence of Temperature and Density Functional Models in *Ab Initio* Molecular Dynamics Simulation of Liquid Water. *J. Chem. Phys.* **2005**, *122*, 014515

(25) Koizumi, K.; Hatakeyama, M.; Boero, M.; Nobusada, K.; Hori, H.; Misonou, T.; Nakamura, S. How Seaweeds Release the Excess Energy from Sunlight to Surrounding Sea Water. *Phys. Chem. Chem. Phys.* **2017**, *19*, 15745–15753

(26) Ikeda, T.; Boero, M.; Terakura, K. Hydration of alkali ions from first principles molecular dynamics revisited *J. Chem. Phys.* **2007**, *126*, 034501

(27) Ikeda, T.; Boero, M. Role of ban der Waals corrections in first principles simulations of alkali metal ions in aqueous solutions. *J. Chem. Phys.* **2015**, *143*, 194510

(28) Ancilotto, F.; Chiarotti, G. L.; Scandolo, S.; Tosatti, E. Dissociation of Methane into Hydrocarbons at Extreme (Planetary) Pressure and Temperature. *Science* **1997**, *275*, 1288-1290

(29) Silvestrelli, P. L.; Parrinello, M. Water Molecule Dipole in the Gas and in the Liquid Phase. *Phys. Rev. Lett.* **1999**, *82*, 3308-3311

(30) Yildirim, T.; Hartman, M.R. Direct Observation of Hydrogen Adsorption Sites and Nanocage Formation in Metal–Organic Frameworks *Phys. Rev. Lett.* **2005**, *95*, 215504

(31) Yang, Q.; Zhong, C. Molecular Simulation of Adsorption and Diffusion of Hydrogen in Metal–Organic Frameworks *J. Phys. Chem. B* **2005**, *109*, 11862-11864

(32) Hohenberg, P.; Kohn, W. Inhomogeneous Electron Gas. *Phys. Rev.* **1964**, *136*, B864-B871

(33) Kohn, W.; Sham, L. J. Self-Consistent Equations Including Exchange and Correlation Effects. *Phys. Rev.* **1965**, *140*, A1133–A1138

(34) Car, R.; Parrinello, M. Unified Approach for Molecular Dynamics and Density-Functional Theory. *Phys. Rev. Lett.* **1985**, *55*, 2471-2474

(35) Perdew, J. P.; Burke, K.; Ernzerhof, M. Generalized Gradient Approximation Made Simple. *Phys. Rev. Lett.* **1996**, *77*, 3865-3868

(36) Grimme, S. Accurate Description of van der Waals Complexes by Density Functional Theory Including Empirical Corrections *J. Comput. Chem.* **2004**, *25*, 1463-1473

(37) Troullier, N.; Martins, J. L. Efficient Pseudopotentials for Plane-Wave Calculations. *Phys. Rev. B* **1991**, *43*, 1993-2006

(38) Schwegler, E.; Grossman, J. C.; Gygi, F.; Galli G. Towards an assessment of the accuracy of density functional theory for first principles simulations of water II *J. Chem. Phys.* **2004**, *120*, 300–311.

(39) Nosé, S. A Molecular Dynamics Method for Simulations in the Canonical Ensemble. *Mol. Phys.* **1984**, *52*, 255-268

(40) Nosé, S. A Unified Formulation of the Constant Temperature Molecular Dynamics Methods. *J. Chem. Phys.* **1984**, *81*, 511-519

(41) Hoover, W. G. Canonical Dynamics: Equilibrium Phase-Space Distributions. *Phys. Rev. A* **1985**, **31**, 1695-1697

(42) Martyna, G. J.; Klein, M. L.; Tuckerman, M. Nosé–Hoover Chains: The Canonical Ensemble via Continuous Dynamics *J. Chem. Phys.* **1992**, *97*, 2635-2643

(43) CPMD, http://www.cpmd.org/, Copyright IBM Corp 1990-2013, Copyright MPI für Festkörperforschung Stuttgart 1997-2001.

(44) Skoulidas, A.; Sholl, D. S. Self-Diffusion and Transport Diffusion of Light Gases in Metal–Organic Framework Materials Assessed Using Molecular Dynamics Simulations *J. Phys. Chem. B* **2005**, *109*, 15760-15768

(45) Bär, N.-K.; Ernst, H.; Jobic, H.; Kärger, J. Combined Quasi-Elastic Neutron Scattering and NMR Study of Hydrogen Diffusion in Zeolites. *Magn. Reson. Chem.* **1999**, *37*, S79-S83

(46) Skoulidas, A. I.; Acherman, D. M.; Johnson, J. K.; Sholl, D. S. Rapid Transport of Gases in Carbon Nanotubes. *Phys. Rev. Lett.* **2002**, *89*, 185901

(47) Lochan, R.; Khaliullin, R. Z.; Head-Gordon, M. Interaction of Molecular Hydrogen with Open Transition Metal Centers for Enhanced Binding in Metal–Organic Frameworks: A Computational Study. *Inorg. Chem.* **2008**, *47*, 4032-4044

(48) Sumida, K.; Stück, D.; Mino, L.; Chai, J.-D.; Bloch, E. D.; Zavorotynska, O.; Murray, L. J.; Dincã, M.; Chavan, S.; Bordiga, S.; Head-Gordon, M.; Long, J. R. Impact of Metal and Anion Substitutions on the Hydrogen Storage Properties of M-BTT Metal–Organic Frameworks. *J. Am. Chem. Soc.* **2013**, *135*, 1083-1091

Acknowledgement

This research was supported by Grant-in-Aid No. 25288012 ", Elements Strategy Initiative to Form Core Research Center" (since 2012), Strategic Programs for Innovative Research (SPIRE), and Computational Material Science Initiative (CMSI), MEXT, Japan. We thank computer facilities ISSP and Information Technology Center, The University of Tokyo and Research Center for Computational Science, Okazaki, Japan. M.B. thanks Pôle HPC and Equipex Equip@Meso at the University of Strasbourg, and Grand Equipement National de Calcul Intensif (GENCI) under allocation DARI-A2 A0040906092. We dedicate this paper to the memory of our friend and colleague Katsuyuki Nobusada.

Graphical TOC Entry